Atmos. Chem. Phys. Discuss., 15, 20811–20850, 2015
www.atmos-chem-phys-discuss.net/15/20811/2015/
doi:10.5194/acpd-15-20811-2015

Atmospheric Chemistry and Physics Discussions

Size distributions of polycyclic aromatic hydrocarbons in urban atmosphere: sorption mechanism and source contributions to respiratory deposition

Y. Lv[1], X. Li[1], T. T. Xu[1], T. T. Cheng[1], X. Yang[1], J. M. Chen[1], Y. Linuma[2], and H. Herrmann[2]

[1]Shanghai Key Laboratory of Atmospheric Particle Pollution and Prevention (LAP3), Department of Environmental Science and Engineering, Fudan University, Shanghai 200032, China
[2]Leibniz-Institut für Troposphärenforschung (IfT), Permoserstr. 15, 04318, Leipzig, Germany

Received: 28 March 2015 – Accepted: 13 July 2015 – Published: 4 August 2015

Correspondence to: X. Li (lixiang@fudan.edu.cn), H. Herrmann (herrmann@tropos.de)

Published by Copernicus Publications on behalf of the European Geosciences Union.

Abstract

Current knowledge on atmospheric particle-phase polycyclic aromatic hydrocarbons (PAHs) size distribution remains incomplete. Information is missing on sorption mechanisms and the influence of the PAHs' sources on their transport in human respiratory system. Here we present the studies systematically investigating the modal distribution characteristics of the size-fractioned PAHs and calculating the source contribution to adverse health effects through inhalation. Aerosol samples with nine size fractions were collected from Shanghai urban air over one year period 2012–2013. A high correlation coefficient existed between measured and predicted values (R^2 = 0.87), indicated that the data worked very well in current study. Most PAHs were observed on the small particles followed with seasonality differences. When normalized by PAHs across particle diameters, the size distribution of PAHs exhibited bimodal patterns, with a peak (0.4–2.1 μm) in fine mode and another peak (3.3–9.0 μm) in coarse mode, respectively. Along with the increasing ring number of PAHs, the intensity of the fine mode peak increased, while coarse mode peak decreased. Plotting of log(PAH/PM) against log(D_p) showed that all slope values were above −1 with the increase towards less-ring PAHs, suggesting that multiple mechanisms, i.e. adsorption and absorption controlled the PAHs on particles, but adsorption played a much stronger role for 5- and 6-ring than 3- and 4-ring PAHs. The mode distribution behavior of PAHs showed that fine particles were major carriers for the more-ring PAHs. Further calculations using inhaling PAHs data showed the total deposition fluxes in respiratory tract were $8.8 \pm 2.0\,\mathrm{ng\,h^{-1}}$. Specifically, fine particles contributed 10–40 % of PAHs deposition fluxes to the alveolar region, while coarse particles contributed 80–95 % of ones to the head region. Estimated lifetime cancer risk (LCR) for people exercised in haze days (1.5×10^{-6}) was bigger than the cancer risk guideline value (10^{-6}). The largest PAHs contribution for LCR mainly came from the accumulation particles. Based on source apportionment results generated by positive matrix factorization (PMF), it was found that the cancer risk caused in accumulated mode mainly resulted from biomass burning (24 %), coal

ACPD
15, 20811–20850, 2015

combustion (25 %) and vehicular emission (27 %). The present results contribute to a mechanistic understanding of PAHs size distribution causing adverse health effects and will help develop some source control strategies or policies by relying on respiratory assessment data.

1 Introduction

Atmospheric PAHs are important contaminants in urban air because of their carcinogenic and mutagenic properties (Li et al., 2006; Garrido et al., 2014). They mainly result from incomplete combustion of carbon-containing materials, and can partition between the gas and the particulate phase (Fernández et al., 2002; Hytönen et al., 2009; Shen et al., 2011). This partitioning strongly depends on particle size distribution, PAH compositions and temperature, and affects the PAHs transport, deposition, degradation processes as well as health impacts. During the partitioning processes, size distributions of PAHs play a critical yet poorly understood role. Of particular importance is the role played by high molecular mass PAHs because most of them are carcinogenic and associated with fine aerosol particles (Akyuz and Cabuk, 2009; Wu et al., 2014). Fine particles loaded with PAHs can travel deep into the human respiratory system, and cause direct health impact, as inhalation exposure depends on particle sizes (Kawanaka et al., 2009; K. Zhang et al., 2012b). Current knowledge on PAHs size distribution remains incomplete. Information is missing on sorption mechanisms and the influence of the PAHs' sources on their transport in human respiratory system. To address these concerns, further studies are necessary and significant.

Over the past decade, numerous measurements on PAHs size distribution have been repeatedly carried out in various areas around the world such as Seoul (Korea) (Lee et al., 2008), Saitama, Okinawa (Japan) (Kawanaka et al., 2004; Wang et al., 2009), Mumbai, Delhi (India) (Venkataraman et al., 1999; Gupta et al., 2011), Barcelona (Spain) (Mesquita et al., 2014), Dresden (Germany) (Gnauk et al., 2011), Birmingham (England) (Delgado-Saborit et al., 2013), Lisbon (Portugal) (Oliveira et al., 2011),

ACPD
15, 20811–20850, 2015

Algiers (Algeria) (Ladji et al., 2014), Beauharnois (Canada) (Sanderson and Farant, 2005), Los Angeles, Massachusetts, Chicago, Claremont (USA) (Venkataraman and Friedlander, 1994; Allen et al., 1996; Offenberg and Baker, 1999; Miguel et al., 2004), Tianjing, Beijing, Guangzhou (China) (Wu et al., 2006; Zhou et al., 2008; Yu and Yu, 2012). These studies, conducted in various countries and cities, showed that most PAHs existed on small particles and had a similar modal distribution for isomers. PAHs size distribution can vary with their releasing sources and change through particle aging processes in the atmosphere (Venkataraman et al., 1994). In order to illustrate the partitioning mechanism of PAHs among particles, Venkataraman et al. (1999) developed the equilibrium adsorption and absorption theory, which explained the predominance of PAHs in nuclei and accumulation mode particles, respectively, but failed to explain the preferential accumulation of less-ring PAHs compared to more-ring PAHs in coarse mode. Allen et al. (1996) proposed that mass transfer by vaporization and condensation helps estimate the size distribution of PAHs. However, this theory does not account for particle deposition and its impact on residence time. Therefore, the mechanisms that govern PAH distributing in a range of particle sizes are not still disputable and require further clarification. The fine particles discussed here can travel deep into the human respiratory system and, for the smallest particles, potentially enter the bloodstream, thus exposing the person to both particles and the particle-bound compounds (Geiser et al., 2005). To solve these problems, the first thing we should figure out the releasing source of PAHs on size-specific particles. However, current studies associated with source apportionment of atmospheric PAHs often do not account for size distribution and their impact on mechanism, deposition and transport in human respiratory system (Chen and Liao, 2006; Sheesley et al., 2009). Understanding PAHs sources attribution on size-specific particles is thus crucial to better describe their atmospheric fate and understand and reduce human exposure.

The present paper aims to contribute to the knowledge base by conducting ambient measurements on aerosol particle size distributions of PAHs in a megacity Shanghai over a one year period. We specifically aim to determine whether there are relation-

ACPD
15, 20811–20850, 2015

ships in the PAHs releasing sources and the involved mechanism associated with adsorption, absorption and inhalation exposure – the main objectives of our research are as follows: (i) to investigate size distributions of atmospheric PAHs; (ii) to elaborate the atmospheric mechanisms and process controlling PAHs distribution among size-resolved particles; (iii) to identify local sources for PAHs on size-specific particles, and (iv) to estimate the source contribution to human respiratory tract through inhalation exposure.

2 Experimental and methods

2.1 Chemicals

All solvents were HPLC grade and bought from Tedia Company Inc, USA. Standard mixtures of PAHs were purchased from Sigma-Aldrich, Shanghai, China. The 16 EPA priority PAHs were investigated, i.e. naphthalene (NAP, 2-ring), acenaphthylene (ANY, 3-ring), acenaphthene (ANA, 3-ring), fluorene (FLU, 3-ring), phenanthrene (PHE, 3-ring), anthracene (ANT, 3-ring), fluoranthene (FLT, 4-ring), pyrene (PYR, 4-ring), benz [a]anthracene (BaA, 4-ring), chrysene (CHR, 4-ring), benzo[b]fluoranthene (BbF, 5-ring), benzo[k]fluoranthene (BkF, 5-ring), benzo[a]pyrene (BaP, 5-ring), dibenz[a, h]anthracene (DBahA, 5-ring), indeno[1,2,3-cd]pyrene (IPY, 6-ring), and benzo[ghi]perylene (BghiP, 6-ring).

2.2 Sampling site

The measurements took place on the rooftop (20 m above the ground) of No. 4 teaching building at Fudan University campus (121.50° E, 31.30° N), approximately 5 km northeast of downtown Shanghai city (elevation about 4 m a.s.l.). There is a Fudan super monitoring station for atmospheric chemistry running all year round. More information on this site can be found in previous studies (X. Li et al., 2011; P. F. Li et al., 2011), and hence only a brief introduction is given. The site is located in a mixed-used neigh-

ACPD
15, 20811–20850, 2015

borhood including many schools, supermarkets and residences. The site is also in close proximity to major Handan Road (about 200 m south) and Guoding Road (about 300 m east); which is the main corridor leading to Xiangyin Tunnel (Huangpu river) and Yangpu bridge. There is always heavy traffic in this area due to the local and cross-border traffics. The main sources of local air pollution at this site include industries emission, household heating, road transport and biomass burning.

2.3 Sample collection and pretreatment

An Anderson 8-stage air sampler (Thermo Electron Corporation, USA) was used to collect aerosol samples with different size ranges, i.e. 10.0 (inlet)–9.0, 9.0–5.8, 5.8–4.7, 4.7–3.3, 3.3–2.1, 2.1–1.1, 1.1–0.7, 0.7–0.4 and < 0.4 µm. Based on the need of this research, the fractions were divided into three modes: aitken (d_p < 0.4 µm), accumulation (0.4 < d_p < 2.1 µm) and coarse (d_p > 2.1 µm) mode. The flow rate of the sampler was controlled at 28.3 L min^{-1}. The average collecting time for each batch of samples was 120 h, and the air volume that passed through the sampler was of 203.8 m^3. The sampling campaign was conducted during the period 12, 2012–12, 2013. A total of 189 size-segregated particle samples were obtained including their corresponding sampling information and meteorological conditions.

Quartz fiber membranes (Whatman QMA, ⌀ 81 mm) were used to collect aerosol particle samples. Before using, the membranes were baked at 450 °C for 4 h, equilibrated at 20 °C and 40 % relative humidity for 24 h, and then weighed. After sampling, the membranes were equilibrated at 20 °C in a desiccator for 24 h and weighed again using the same procedure. Then, the membranes were stored in freezers at −20 °C until they were extracted. Extraction was performed as soon as possible before some less-ring PAHs volatilized. The procedure applying for PAHs pretreatment was Soxhlet extraction. Briefly, the filter samples were put in a Soxhlet apparatus and extracted in a refluxing dichloromethane/hexane (1 : 1, *v*/*v*) for 36 h. The temperature was controlled at 69 °C. After the extraction was completed, the contents were filtered

ACPD
15, 20811–20850, 2015

by a 0.45 µm PTFE membrane to remove insoluble particles, and then concentrated to exactly 2 mL by rotary evaporator and under gentle nitrogen stream. The final extracts were stored in the refrigerator for further quantitative and qualitative analysis. The detailed pretreatment procedure could be found elsewhere (Mai et al., 2003).

2.4 Analytical procedure

All samples were quantified for 16 PAHs by an Agilent 7890A Series GC coupled to an Agilent 7000B Triple Quadrupole MS (GC/MS/MS, Agilent Technologies Inc., USA) operated in EI mode. The analysis was performed using the Multiple Reaction Monitoring (MRM) procedure. The separation was achieved with a HP-5MS capillary column (30 m × 0.25 mm i.d. × 0.25 µm). The GC oven temperature was programmed from 70 °C (hold for 2 min) to 280 °C at 15 °C min^{-1}, and finally 310 °C at 5 °C min^{-1} with a hold of 1 min. The total program time was 23 min. The temperatures of the injector, ion source and transfer line were controlled at 310, 300 and 310 °C, respectively. Analyses were carried out in the constant flow mode. Ultra high purity Helium (99.999 %) was applied as carrier gas with the flow rate of 1.2 mL min^{-1}. Nitrogen was used as collision gas.

Matrix-matched calibration curves (5 to 1000 ng mL^{-1}) were obtained for all compounds on the GC/MS/MS instrument, by plotting the compound concentration vs. the peak area and determining the R^2 using weighted linear regression (1/x) with the quantitative analysis software for GC/MS/MS. Limits of detection (LODs) and limits of quantification (LOQs) were measured based on signal to noise ratio at about 3 and 10, respectively. The average blank value is subtracted from each signal being above the LOD. Recovery tests were used to estimate possible losses of PAHs during the extraction process. The blank filters were spiked with the standard mixture and gone through the same procedures for analysis. The results (n = 3) showed that the mean recoveries ranged 70 to 100 % for all PAHs. All concentrations reported were corrected by their respective recovery percentage.

ACPD
15, 20811–20850, 2015

2.5 Statistical analysis

Statistical analysis was carried out using partial least-squares regression (PLS) procedure in the SIMCA-P software (Version 11.5, Umetrics Inc., Umeå, Sweden). The size-segregated particles and corresponding PAHs contents are respectively used as Y variables and X variables in PLS model. All variables were centred and scaled to unit variance before the analysis. Thereby all variables contributed with equal weight to the model. An important parameter in PLS analysis is the cross-validation correlation coefficient (O^2), which is calculated from predicted residual sum of squares and can give an evaluation of the model's predictive ability in SIMCA (Lindgren et al., 1995). A large O^2 value (> 0.5) means that the PLS model has a predictivity better than chance. In addition, the observed vs. predicted plot to give a more direct displays for the values of the selected response. The correlation coefficient (R^2) between observed and predicted can be utilized for the evaluation of the goodness of model fit. Generally, R^2 value greater than 0.8 indicates PLS model constructed in software fits well with the data.

2.6 PMF source apportionment

Source apportionment of the size-segregated PAHs was performed using Positive Matrices Factorization (PMF). In the following, PMF will be shortly outlined (Larsen and Baker, 2003; Ma et al., 2010). By analyzing measured concentrations at receptor sites, the method can identify a set of factors which can be taken to represent major emission sources (Paatero and Tapper, 1994). PMF models are expressed as follows:

$$x_{ij} = \sum_{k=1}^{p} g_{ik} f_{kj} + e_{ij} \quad (1)$$

Where X is a data matrix of i by j dimension, in which i is the number of the size-segregated particle sample and j is the number of the measured PAH species. f_{kj} is

ACPD
15, 20811–20850, 2015

the concentration of the jth PAH species in the emissions from the kth source; g_{ik} is the contribution of the kth source to ith particle sample. e_{ij} is the portion of the measured concentration that cannot be explained by the model.

By incorporating an uncertainty for each observation u_{ij}, the PMF solution can minimize the objective function Q (Eq. 2),

$$Q = \sum_{i=1}^{n} \sum_{j=1}^{m} \left[\frac{x_{ij} - \sum_{k=1}^{p} g_{ik} f_{kj}}{u_{ij}} \right]^2 \quad (2)$$

The PMF model requires data on measured PAH concentrations for all samples, together with information on the associated uncertainties. The confidence of results can be maintained by adjusting the data uncertainties. This allows us to lower the importance of these data through the least squares fit. The work presented here is the US EPA PMF version 3.0. Please find more information about these on US EPA website (http://www.epa.gov/heasd/research/pmf.html).

2.7 Human respiratory risk assessment

In order to evaluate the human respiratory potential of the size-segregated PAHs, we adopted an International Commission on Radiological Protection (ICRP) model (ICRP, 1994) for these. Based on inhaled particles sizes, the respiratory tract is divided into three main regions: head, tracheobronchial, and alveolar region. The PAH concentrations were loaded into the ICRP model to calculate the deposition efficiency and flux of inhaled PAHs.

Lifetime cancer risk (LCR) were applied to assess the cancer risk associated with exposure to the size-segregated PAHs through inhalation of ambient particles (Kawanaka et al., 2009; K. Zhang et al., 2012b). The LCR can then be calculated by the formula

ACPD
15, 20811–20850, 2015

(US EPA, 1989):

$$LCR = EI \times ED \times CSF/(AT \times BW) \quad (3)$$

where EI is the estimated inhalation rate ($mg\,d^{-1}$) which is calculated by deposition fluxes ($mg\,h^{-1}$) and daily exposure time ($12\,h\,d^{-1}$), ED is the exposure duration for an adult (30 years), CSF is the inhalation cancer slope factor ($(mg\,kg^{-1}\,d^{-1})^{-1}$), BW is the body weight (~ 60 kg), and AT is the average lifetime (70 years). As suggested by the OEHHA, a value of 3.9 of BaP was usually applied as a recommended value for the calculation of CSF in LCR formula (Liu et al., 2007).

3 Results and discussion

3.1 Occurrence and size distribution of PAHs

Figure 1 presents the time trend of the total PAHs, size-segregated particles, visibility and relative humidity (RH) during the sampling period. Results show high PAHs episodes coincide with high PM levels, along with the low RH and low visibility. Average total PAH concentrations adsorbed on particles range from 41.6 to 66.6 $ng\,m^{-3}$ (average: 48.7 $ng\,m^{-3}$). The concentration of total particles during the period varies from 54.8 to 209.6 $\mu g\,m^{-3}$ (average: 122.8 $\mu g\,m^{-3}$). Among them, the daily $PM_{2.5}$ concentration is 61.8 $\mu g\,m^{-3}$, which is obviously higher than the annual (daily) national air quality standard of 10 (25) $\mu g\,m^{-3}$ set by the World Health Organization (WHO 2005). Most particles mass is found in the accumulation mode size ranges (0.4–2.1 µm). Fine particles are typically higher than coarse particles in Shanghai air. This finding is consistent with particle size distribution in Shanghai (Wang et al., 2014). The $PM_{2.5}/PM_{10}$ ratio of (50±8 %) suggests that the anthropogenic component of particle matter as represented by the PM_1 fraction is significant in the studied area (Theodosi et al., 2011).

For the investigation of seasonal trends, the PAHs data is divided into 4 seasonal groups, i.e. spring (March to May), summer (June to August), autumn (September to

ACPD
15, 20811–20850, 2015

November) and winter (December to February). There is a distinct seasonal cycle for total PAHs with higher values in winter than in summer (Fig. 2) corresponding to temperature differences first of all. The amplitude of the cycles depends on particle size, for example, PAHs concentrations are generally higher in the fine particles ($d_p < 2.1$ µm) than in the coarse particles ($d_p > 2.1$ µm). This fact indicates that total PAHs are mainly adsorbed onto small particles due to their extremely large available surface. Seasonal differences may be related to ambient temperature and the different volatilities of PAH compounds. This seasonal variation is similar to the findings in other places for atmospheric PAHs (van Drooge and Ballesta, 2009; Ma et al., 2010). The different distribution patterns of PAHs in fine and coarse particles may be attributed to different emission mechanisms of PAHs in urban areas. More details will be included in the following detailed discussion about mode analysis and source attribution associated with size distribution.

Some empirical evidence suggests that PAHs with similar molecular weights or ring numbers maybe have similar aerosol particle size distributions (Allen et al., 1996; Duan et al., 2005, 2007). Based on their volatility and aromatic ring numbers, 16 PAHs are divided into four groups, i.e. 3- to 6-ring PAHs. To better describe PAHs distributions, the commonly used way is to plot a log-log chart, i.e., $dC/d\log D_p$ is plotted against D_p (Particle diameter) on the log scale where dC is the PAHs concentrations in each particle size bin and $d\log D_p$ is the size width of each impactor channel (Kawanaka et al., 2004; Venkataraman and Friedlander, 1994; Venkataraman et al., 1999). Figure 3 clearly demonstrates that the size distribution of PAHs exhibited bimodal patterns, with a peak (0.4–2.1 µm) in fine mode and another peak (3.3–9.0 µm) in coarse mode. The peak intensities vary towards larger PAHs, i.e. the peak in accumulation mode becomes more predominant, while another one in coarse mode becomes weaker and even disappears for 5- and 6-ring PAHs. This is because less volatile compounds preferentially condense on fine particles and more volatile PAH species are inhibited on smaller particles because of the Kelvin effect (Hien et al., 2007; Keshtkar and Ashbaugh, 2007). This kind of distribution mode that appears in Shanghai is similar to those found in

ACPD
15, 20811–20850, 2015

Mumbai, India (Venkataraman et al., 1999), but not same in Boston, MA (Allen et al., 1996). From the results of PAHs distribution, one can also obtain important implication for health hazards via inhalation. Since the majority of larger PAHs has mutagenic and/or carcinogenic properties and almost exclusively exists on fine particles which can travel deep into the human respiratory system and hence can cause a serious health risk through exposing a person to both particles and the loaded carcinogenic PAHs (Kameda et al., 2005).

3.2 Atmospheric processing and partitioning mechanisms

Previous studies on atmospheric process of PAHs mainly focus on gas/particle partitioning (R. Zhang et al., 2012; McWhinney et al., 2013), but few studies focus on the aerosol particle size distribution of PAHs. To further understand the significance of size dependency during the PAHs atmospheric processing, size-fractionated PAHs data acquired in the present study are used to assess the PAHs partitioning among different particle sizes.

Empirical evidences suggest mass ratios of PAH to particulate matter (PAH/PM) can provide some valuable implications for PAHs atmospheric process. PAHs that released from incomplete combustion of organic material are mainly associated with size-segregated aerosol particles through adsorption and absorption. The size-resolved PAHs would be involved in the aging process of aerosol. During this process, atmospheric PAHs could be photooxidized to form secondary organic aerosol (SOA), increasing organic fine particulate matter through either self-nucleation or gas-particle partitioning (Kavouras et al., 1999; Kamens et al., 1999; Yu et al., 1999; Kamens and Jaoui, 2001; Chan et al., 2009). That means that the aging process will reduce the value of PAH/PM (Duan et al., 2005). Figure 4 shows the variation of PAH/PM values by size across all the samples demonstrating that values for the ratio PAH/PM range between 0.01 and 0.1 depending on PAH species characteristics. In general, PAH/PM ratios decrease gradually towards particles with the bigger size. However, it should be noted that 5- and 6-ring PAH/PM ratios showed a little increasing fluctuation during the

ACPD
15, 20811–20850, 2015

size range 2.1–5.8 µm. The reasons for this phenomenon are unclear but may be related to long repartitioning process of low volatile 5- and 6-ring PAHs in coarse particles due to the lower vapour pressures (Bi et al., 2005), or mass of PM in this size range decreased by dry and wet deposition or forming larger particles through coagulation.

The isomer ratio of a more reactive PAH to a stable PAH, such as BaA/Chr and BaP/BeP, can be employed to illustrate the PAHs atmospheric fate (Ding et al., 2007). During this transport process, BaA and BaP are expected to degrade more easily than their isomers, so the ratios will be modified by their strong reactivity. Naturally, the values would degrade over transport time (Duan et al., 2005). Figure 5 reveals the variations of BaA/Chr by size across all the samples. Apart from a few particular values during the size range 5.8–10.0 µm, the majority declines with the increase of particle size. This trend is approximately in accord with the changes of total PAH/PM across all samples. This indicates that PAH species are indeed involved in the processes of changing particle size distribution or aerosol aging, and can provide some information about the aging degree to a certain extent. Nevertheless, aerosol aging estimated by size-fractionated PAHs in the present study still meets some uncertainties because of the scarcity of some correlative variabilities such as particle increase velocities and meteorological conditions. Again, only size distribution of PAHs during the atmospheric process are estimated in the present study, therefore further studies (e.g., particle and PAH formation models and corresponding influencing mechanisms) are needed to provide more insights into the particle aging associated with PAHs. Although the present study does not look directly at the partitioning process, it has taken advantage of the size-fractionated PAHs data to examine the governing mechanisms for aerosol size distribution.

Currently, the reliable mechanisms for controlling PAHs distribution in size-resolved particles include adsorption to nucleus particles, adsorption and absorption to accumulation particles, and multilayer adsorption on coarse particles (Venkataraman et al., 1999). Adsorption and absorption depend respectively on available particle surface area and organic mass. If PAHs are firstly associated with the particle surface, the

ACPD
15, 20811–20850, 2015

PAH/PM mass ratio will show a 1/*D*p dependence (assuming particles are spherical), and then will generate a straight line of slope −1 on a log vs. log axis (Venkataraman et al., 2002). Plotting of log(PAH/PM) against log(D_p) showed that all slope values were above −1 with the decrease towards to the more-ring PAHs (Fig. 6), suggesting that multiple mechanisms, i.e. adsorption and absorption controlled the PAHs on particles, but adsorption played a much stronger role for 5- and 6-ring than 3- and 4-ring PAHs. This might be caused by the relatively lower volatility of 5- and 6-ring PAHs compared to smaller ones letting these compounds adjust to multiple adsorptive equilibrium more slowly. Moreover, chemical affinities maybe also play an important role in adsorption process. Most more-ring PAHs have strong hydrophobicity and tend to affiliate with small particles because they can provide large surface areas (Venkataraman et al., 1999). Such an explanation, however, can not adequately account for the PAHs equilibrium mechanisms observed in the present study. Perhaps in fact more-ring PAHs do not attain equilibrium due to slow mass transfer, but they reach steady state between the gaseous and particulate phases (Yu and Yu, 2012).

3.3 Statistical analysis

In an attempt to understand how the alterations in particle size may lead to variations in PAH species, we built a statistical model using PLS regression based on all PAHs data. After calculating five components are adopted because they can give the most stable results and easily interpretable factors. The number of components in PLS is also consistent with the PMF results, as discussed in the next section. By plotting the observed (measured) values vs. the predicted values, for the particle sizes included in the models, we got a goodness of fit with R^2 = 0.87, a goodness of prediction with Q^2 = 0.80, and the root mean square error of the fit for observations in a RMSEE value of 0.87. Figure 7 shows the observed vs. predicted plot for the model. The plot performs well in predicting the size-resolved PAHs over the size range between 0.4 and 10 µm. There is no systematic underestimation (or overestimation) and most points fall close to 45° line. The results achieve the desired separation without overlap among eight

ACPD
15, 20811–20850, 2015

particle size ranges. Most variations of size-resolved PAHs, i.e., up to 80 % can be predicted by the parameterization. The model can explain 91 % of X, 87 % of Y and predict 80 % of Y. These predictions are not de novo predictions, since all the data are part of the observed set. Nevertheless, these predicted results do validate the model effectiveness and the measured data reliability.

Similarities between PAHs profiles at the two adjacent sizes can be further identified by coefficient of divergence (CD), which is a self-normalizing parameter used to evaluate the divergence degree of two sets of data (Kong et al., 2012). CD is determined as follows:

$$\mathrm{CD}_{jk} = \sqrt{\frac{1}{p}\sum_{i=1}^{p}\left(\frac{x_{ij}-x_{ik}}{x_{ij}+x_{ik}}\right)^2} \quad (4)$$

Where j and k stand for the two adjacent particles fractions, p was the number of investigated PAHs, and x_{ij} and x_{ik} represented the concentrations of PAHs species i for size j and k (Kong et al., 2011). CD is ranging from 0 to 1. A low CD value (< 0.2) indicates a high level of homogeneity in PAHs distribution between adjacent sizes, while CD values larger than 0.2 indicate heterogeneous PAHs spatial distribution (Wilson et al., 2005). Figure 8 shows the PAHs CD diagrams that are characterized by color block. For the comparison between the adjacent sizes, the CD_{jk} values were all less than 0.2 except $\mathrm{CD}_{0.4,\,0.4--0.7}$ (0.26) and $\mathrm{CD}_{1.1--2.1,\,2.1--3.3}$ (0.31), indicating that PAHs in the two adjacent sizes fractions show a high spatial homogeneity of the source factor contributions.

3.4 Emission source of size-fractionated PAHs

The different distribution patterns of PAHs in fine and coarse particles may be attributed to different emission mechanisms of PAHs. By applying the PMF model, five main source factors have been chosen in this study after comparing three or four main factors. Five identified sources for the PAHs are respectively associated with vehicular

ACPD
15, 20811–20850, 2015

emission, biomass burning, coal combustion, petroleum residue and air–surface exchange. Figure 9 shows the profiles for all factors. Factor 1 presents a profile with high factor loadings for 5- and 6-ring PAHs, i.e. B(b + k)F, BaP, IPY, DBahA and BghiP. These high molecular weight PAHs are reported as dominant in vehicle emissions (Bostrom et al., 2002; Ravindra et al., 2008). BbF and BkF are attributed to diesel motor vehicle emissions, while BaP and BaA are attributed to gasoline and diesel markers (Harrison et al., 1996; Sofowote et al., 2008). Thus, this factor is named as vehicular emissions without distinguishing between diesel and gasoline releasing. Factor 2 is dominated by high loadings of PHE, Flu and BbF and moderate loadings of Chr, BkF, BaA, IP and BghiP. This factor profile mainly came from biomass burning that has been described in the previous study (Poulain et al., 2011). As the occurrence of biomass burning in Shanghai city is normally low, this source is most likely from long range transport, rather than from local releasing. Factor 3 is characterized by B(b + k)F, CHR, BaA and BghiP. These compounds have been reported by different authors as coal combustion source markers (Yang et al., 2002; Lin et al., 2011). Although in Shanghai, natural gas is one of the main fuels used for domestic heating, there are still central heating systems using coal and petrol-derived fuels. Moreover, the influence of power plant, soking, steel and iron industries using coal as fuel could be also reflected on this factor. Factor 4 is mainly defined by 4- and 5-ring PAHs. High levels of these compounds, especially for PHE are associated with crude oil or refined petroleum emission and their degradation products (Zakaria et al., 2002). So this factor is likely to represent petroleum residue, or the derivatives from oil spill, the leakage from vehicles, and the discharge from municipal and industrial wastewater, etc. Factor 5 is more influenced by 2- and 3-ring PAHs. These less-ring PAHs are favored in air–surface exchange (Gigliotti et al., 2002). The "exchange" here means that the aged PAHs are probably released into the atmosphere again from contaminated soil or wastewater, and then adsorbed later by the particles. Moreover, they are also transported to here through long ranges and finally deposit on particle surfaces. Thus, factor 5 is ascribed to air–surface exchange.

ACPD
15, 20811–20850, 2015

Based on the source apportionment results, the contributions of each factor are summarized in Fig. 10. As expected, the results are quite different between particle sizes. Coal combustion and biomass burning accounted for 29 and 29 % of total PAHs in accumulation mode aerosols, whereas they are 12 and 13 % in coarse mode aerosols. Their contribution for particulate PAHs significantly decreases with increasing particle size due to large deposition velocities of large particles. Air–surface exchange and petroleum residue account for 9 and 10 % of total PAHs in accumulation mode aerosols whereas they are 30 and 27 % in coarse mode aerosols. Note that the concentrations of vehicle-derived PAHs (vehicular emission) are almost constant through the year, i.e. it is 22 % of total PAHs in accumulation mode aerosols whereas it is 18 % of total PAHs in coarse mode aerosols. When taking the size distribution of the PAH into consideration, it can conclude easily interpretable main emission sources for PAHs. As discussed above, most PAHs are characterized by a main peak in accumulation mode, suggesting that high concentration of PAHs occurred in fine particles. Additionally, concentrations of total PAHs in fine particles contribute to 80 % of total concentrations in PM. Apparently, the presence of sources at or close to fine particulate level should be collectively responsible for this observation. Consequently, vehicle exhaust, coal combustion and biomass burning are deemed three appreciable source of PAHs. Moreover, multiple emission mechanisms, i.e. vehicle exhaust, coal combustion and biomass burning tend to contribute fine particles, which largely adsorb PAHs that generated at the same time due to the large specific surface area, and results in significantly higher concentrations of PAHs in fine particles than in coarse particles.

3.5 Respiratory exposure to PAHs

In order to assess deposition efficiency and flux of size-resolved PAHs in the human respiratory tract, we applied a so-called International Commission on Radiological Protection (ICRP) model (1994). More details on calculating from the model are included elsewhere (K. Zhang et al., 2012a; Kawanaka et al., 2009). Commonly, the respiratory tract is divided into three deposition regions: head airway (HA), tracheobronchial

ACPD
15, 20811–20850, 2015

(TB), and alveolar region (AR). The breath rate of normal people was considered at 0.45 $m^3 h^{-1}$. Figure 11 shows the deposition fluxes of size-resolved PAHs and their relative contributions in the head, tracheobronchial and alveolar regions. Apparently, we can find a flux peak value in accumulation mode particles (1.1–2.1 µm), similar to size distribution of PAHs as described previously (see Sect. 3.1). The total PAHs deposition fluxes are 8.8 ± 2.0 ng h^{-1}. The mean value (8.8 ng h^{-1}) is 2.4 times higher than that in indoor air of an urban community of Guangzhou, China (3.7 ng h^{-1}) (K. Zhang et al., 2012a). Conversely, the intake rate of total PAHs is much lower than that for a common traffic police in Beijing (280 ng h^{-1} calculated by the respiratory rate of 0.83 $m^3 h^{-1}$) (Liu et al., 2007). In addition, through calculating the relative abundance of PAHs in each region, we can find that they change significantly over particle sizes. As particle size increases, the relative abundance of PAHs in the head region increases, while in alveolar region decreases. Note that the relative abundance of PAHs in tracheobronchial region is almost constant across all particle sizes, i.e. it is 6 % from accumulation mode particles whereas it is 4 % from coarse mode particles. These results indicate that coarse particles only contribute PAHs in head region, while small particles are major contributors to PAHs deposition in alveolar region. Furthermore, these fine or ultrafine particles can also pass human lung rapidly into the systematic circulation, which may cause systematic exposure to PAHs (Nemmar et al., 2002).

Evaluating respiratory exposure incorporates considering the deposition efficiency of size-resolved PAHs. Deposition efficiency represents the deposition effectiveness of atmospheric PAHs in human respiratory tract. The efficiency can then be calculated by the formula of ICRP model. Figure 12 shows the regional deposition efficiency of total PAHs across particle sizes. Generally, the total deposition efficiency of PAHs is found to increase with the particles size increases. However, in the alveolar region, the deposition efficiencies of total PAHs monotonously increased towards the smaller particles. This result suggests that the smaller particle can penetrate the respiratory tract and travel into the deeper alveolar region. This, combined with the fact that most more-

ACPD
15, 20811–20850, 2015

ring PAHs tend to adsorb on smaller particles, makes it more important for potential damage.

One can utilize the LCR to estimate the exposure of PAHs through inhalation of ambient particles. From Fig. 13, the variations of the LCR from normal (breath rate: 0.45 $m^3 h^{-1}$) and exercising people (breath rate: 0.83 $m^3 h^{-1}$) across particle sizes during haze and non-haze periods can be identified. The size distribution of LCR is also unimodal with the maximum in the 1.1–2.1 µm particle fraction. LCR from the PAHs in accumulation mode particles contribute mainly 54 % of total PAHs. These data show that accumulation particles are major carriers for carcinogenic PAHs. Through the LCR calculation from the exposure to particulate PAHs, we can obtain that the LCR value of a normal people is 6.3(±0.8) $\times 10^{-7}$ during the Shanghai haze period, which is lower than the cancer risk guideline value (10^{-6}) (US EPA, 1989). Here, it should be emphasized that LCR depended strongly on the respiratory rate (0.45 $m^3 h^{-1}$ was utilized for normal condition). If another average respiratory rate of 0.83 $m^3 h^{-1}$ (for exercise people) applied by Liu et al. (Liu et al., 2007) was also used here, total LCR would be 1.2(±0.2) $\times 10^{-6}$, which approached or exceeded the cancer risk guideline value, especially in severe haze days the value peaked at almost 1.5×10^{-6}. Note that this value is only from the size-resolved particulate PAHs, and responsible to part of respiratory risk to atmospheric PAHs. If the gaseous PAHs were also taken into account, the cancer risk would probably be even much bigger. Furthermore, in combination with previous PMF source analysis on size-fractionated PAHs, the higher cancer risk caused in accumulated mode mainly resulted from biomass burning (24 %), coal combustion (25 %) and vehicular emission (27 %). Consistently with our results, epidemiological studies reported that smaller particles could give rise to larger risk of cardiovascular toxicity through breathing (Pope et al., 2009). Thus, it appears to be important to perform more restrict control on smaller particles emission, particularly aiming at the reducing their releasing sources.

ACPD
15, 20811–20850, 2015

4 Summary and conclusions

The overall conclusion of the present study is that it systematically investigated the modal distribution characteristics of PAHs in the Shanghai urban atmosphere and determined the source contribution to adverse health effects through inhalation. It was found that the PAHs size distribution exhibited a bimodal pattern, with one peak (0.4–2.1 µm) in the fine mode and another peak (3.3–9 µm) in the coarse mode. This present study proposes the multiple adsorption and absorption mechanisms controlling the behavior and fate of PAHs particles considered as a function of size. Further calculations using inhaling particle-bound PAHs data showed the estimated LCR were bigger than the cancer risk guideline value (10^{-6}), especially for people exercising during haze days (1.5×10^{-6}). The largest contribution for LCR mainly came from PAHs on accumulation particles, and mainly resulted from biomass burning (24 %), coal combustion (25 %) and vehicular emission (27 %). The findings presented here could provide a preliminary data for developing effective strategies for source control.

Acknowledgements. This work was supported by the National Natural Science Foundation of China (Nos. 21177025, 21377028, 41475109), the Excellent Academic Leader Program (No. 14XD1400600), FP720 project (AMIS, IRSES-GA-2011) and the Major Research Project (No. 12DJ1400100) of Science and Technology Commission of Shanghai Municipality.

References

Akyuz, M. and Cabuk, H.: Meteorological variations of $PM_{2.5}$/ PM_{10} concentrations and particle-associated polycyclic aromatic hydrocarbons in the atmospheric environment of Zonguldak, Turkey, J. Hazard. Mater., 170, 13–21, 2009.

Allen, J. O., Dookeran, K. M., Smith, K. A., Sarofim, A. F., Taghizadeh, K., and Lafleur, A. L.: Measurement of polycyclic aromatic hydrocarbons associated with size-segregated atmospheric aerosols in Massachusetts, Environ. Sci. Technol., 30, 1023–1031, 1996.

ACPD
15, 20811–20850, 2015

Bi, X., Sheng, G., Peng, P. A., Chen, Y., and Fu, J.: Size distribution of *n*-alkanes and polycyclic aromatic hydrocarbons (PAHs) in urban and rural atmospheres of Guangzhou, China, Atmos. Environ., 39, 477–487, 2005.

Bostrom, C. E., Gerde, P., Hanberg, A., Jernstrom, B., Johansson, C., Kyrklund, T., Rannug, A., Tornqvist, M., Victorin, K., and Westerholm, R.: Cancer risk assessment, indicators, and guidelines for polycyclic aromatic hydrocarbons in the ambient air, Environ. Health Persp., 110, 451–488, 2002.

Chan, A. W. H., Kautzman, K. E., Chhabra, P. S., Surratt, J. D., Chan, M. N., Crounse, J. D., Kürten, A., Wennberg, P. O., Flagan, R. C., and Seinfeld, J. H.: Secondary organic aerosol formation from photooxidation of naphthalene and alkylnaphthalenes: implications for oxidation of intermediate volatility organic compounds (IVOCs), Atmos. Chem. Phys., 9, 3049–3060, doi:10.5194/acp-9-3049-2009, 2009.

Chen, S. C. and Liao, C. M.: Health risk assessment on human exposed to environmental polycyclic aromatic hydrocarbons pollution sources, Sci. Total Environ., 366, 112–123, 2006.

Delgado-Saborit, J. M., Stark, C., and Harrison, R. M.: Use of a versatile high efficiency multiparallel denuder for the sampling of PAHs in ambient air: gas and particle phase concentrations, particle size distribution and artifact formation, Environ. Sci. Technol., 48, 499–507, 2013.

Ding, X., Wang, X. M., Xie, Z. Q., Xiang, C. H., Mai, B. X., Sun, L. G., Zheng, M., Sheng, G. Y., Fu, J. M., and Pöschl, U.: Atmospheric polycyclic aromatic hydrocarbons observed over the North Pacific Ocean and the Arctic area: spatial distribution and source identification, Atmos. Environ., 41, 2061–2072, 2007.

Duan, J. C., Bi, X. H., Tan, J. H., Sheng, G. Y., and Fu, J. M.: The differences of the size distribution of polycyclic aromatic hydrocarbons (PAHs) between urban and rural sites of Guangzhou, China, Atmos. Res., 78, 190–203, 2005.

Duan, J. C., Bi, X. H., Tan, J. H., Sheng, G. Y., and Fu, J. M.: Seasonal variation on size distribution and concentration of PAHs in Guangzhou city, China, Chemosphere, 67, 614–622, 2007.

Fernández, P., Grimalt, J. O., and Vilanova, R. M.: Atmospheric gas-particle partitioning of polycyclic aromatic hydrocarbons in high mountain regions of Europe, Environ. Sci. Technol., 36, 1162–1168, 2002.

Garrido, A., Jimenez-Guerrero, P., and Ratola, N.: Levels, trends and health concerns of atmospheric PAHs in Europe, Atmos. Environ., 99, 474–484, 2014.

ACPD
15, 20811–20850, 2015

Geiser, M., Rothen-Rutishauser, B., Kapp, N., Schurch, S., Kreyling, W., Schulz, H., Semmler, M., Hof, V. I., Heyder, J., and Gehr, P.: Ultrafine particles cross cellular membranes by nonphagocytic mechanisms in lungs and in cultured cells, Environ. Health Persp., 113, 1555–1560, 2005.

Gigliotti, C. L., Brunciak, P. A., Dachs, J., Glenn, T. R., Nelson, E. D., Totten, L. A., and Eisenreich, S. J.: Air-water exchange of polycyclic aromatic hydrocarbons in the New York-New Jersey, Usa, Harbor Estuary, Environ. Toxicol. Chem., 21, 235–244, 2002.

Gnauk, T., Muller, K., Bruggemann, E., Birmili, W., Weinhold, K., van Pinxteren, D., Loschau, G., Spindler, G., and Herrmann, H.: A study to discriminate local, urban and regional source contributions to the particulate matter concentrations in the city of Dresden, Germany, J. Atmos. Chem., 68, 199–231, 2011.

Gupta, S., Kumar, K., Srivastava, A., Srivastava, A., and Jain, V. K.: Size distribution and source apportionment of polycyclic aromatic hydrocarbons (PAHs) in aerosol particle samples from the atmospheric environment of Delhi, India, Sci. Total Environ., 409, 4674–4680, 2011.

Harrison, R. M., Smith, D. J. T., and Luhana, L.: Source apportionment of atmospheric polycyclic aromatic hydrocarbons collected from an urban location in Birmingham, UK, Environ. Sci. Technol., 30, 825–832, 1996.

Hien, T. T., Thanh, L. T., Kameda, T., Takenaka, N., and Bandow, H.: Distribution characteristics of polycyclic aromatic hydrocarbons with particle size in urban aerosols at the roadside in Ho Chi Minh City, Vietnam, Atmos. Environ., 41, 1575–1586, 2007.

Hytönen, K., Yli-Pirilä, P., Tissari, J., Gröhn, A., Riipinen, I., Lehtinen, K. E. J., and Jokiniemi, J.: Gas–particle distribution of PAHs in wood combustion emission determined with annular denuders, filter, and polyurethane foam adsorbent, Aerosol Sci. Tech., 43, 442–454, 2009.

International Commission on Radiological Protection (ICRP): Human respiratory tract model for radiological protection, Publication 66, Elsevier Science, Oxford, UK, 1994.

Kameda, Y., Shirai, J., Komai, T., Nakanishi, J., and Masunaga, S.: Atmospheric polycyclic aromatic hydrocarbons: size distribution, estimation of their risk and their depositions to the human respiratory tract, Sci. Total Environ., 340, 71–80, 2005.

Kamens, R., Jang, M., Chien, C. J., and Leach, K.: Aerosol formation from the reaction of alpha-pinene and ozone using a gas-phase kinetics aerosol partitioning model, Environ. Sci. Technol., 33, 1430–1438, 1999.

ACPD
15, 20811–20850, 2015

Kamens, R. M. and Jaoui, M.: Modeling aerosol formation from alpha-pinene plus NOx in the presence of natural sunlight using gas-phase kinetics and gas-particle partitioning theory, Environ. Sci. Technol., 35, 1394–1405, 2001.

Kavouras, I. G., Mihalopoulos, N., and Stephanou, E. G.: Secondary organic aerosol formation vs. primary organic aerosol emission: in situ evidence for the chemical coupling between monoterpene acidic photooxidation products and new particle formation over forests, Environ. Sci. Technol., 33, 1028–1037, 1999.

Kawanaka, Y., Matsumoto, E., Sakamoto, K., Wang, N., and Yun, S. J.: Size distributions of mutagenic compounds and mutagenicity in atmospheric particulate matter collected with a low-pressure cascade impactor, Atmos. Environ., 38, 2125–2132, 2004.

Kawanaka, Y., Tsuchiya, Y., Yun, S.-J., and Sakamoto, K.: Size distributions of polycyclic aromatic hydrocarbons in the atmosphere and estimation of the contribution of ultrafine particles to their lung deposition, Environ. Sci. Technol., 43, 6851–6856, 2009.

Keshtkar, H. and Ashbaugh, L. L.: Size distribution of polycyclic aromatic hydrocarbon particulate emission factors from agricultural burning, Atmos. Environ., 41, 2729–2739, 2007.

Kong, S., Lu, B., Ji, Y., Bai, Z., Xu, Y., Liu, Y., and Jiang, H.: Distribution and sources of polycyclic aromatic hydrocarbons in size-differentiated re-suspended dust on building surfaces in an oilfield city, China, Atmos. Environ., 55, 7–16, 2012.

Kong, S. F., Shi, J. W., Lu, B., Qiu, W. G., Zhang, B. S., Peng, Y., Zhang, B. W., and Bai, Z. P.: Characterization of PAHs within PM_{10} fraction for ashes from coke production, iron smelt, heating station and power plant stacks in Liaoning Province, China, Atmos. Environ., 45, 3777–3785, 2011.

Ladji, R., Yassaa, N., Balducci, C., and Cecinato, A.: Particle size distribution of *n*-alkanes and polycyclic aromatic hydrocarbons (PAHS) in urban and industrial aerosol of Algiers, Algeria, Environ. Sci. Pollut. R., 21, 1819–1832, 2014.

Larsen, R. K. and Baker, J. E.: Source apportionment of polycyclic aromatic hydrocarbons in the urban atmosphere: a comparison of three methods, Environ. Sci. Technol., 37, 1873–1881, 2003.

Lee, J. Y., Shin, H. J., Bae, S. Y., Kim, Y. P., and Kang, C. H.: Seasonal variation of particle size distributions of PAHs at Seoul, Korea, Air Qual. Atmos. Hlth., 1, 57–68, 2008.

Li, J., Zhang, G., Li, X. D., Qi, S. H., Liu, G. Q., and Peng, X. Z.: Source seasonality of polycyclic aromatic hydrocarbons (PAHs) in a subtropical city, Guangzhou, South China, Sci. Total Environ., 355, 145–155, 2006.

ACPD
15, 20811–20850, 2015

Li, P. F., Li, X., Yang, C. Y., Wang, X. J., Chen, J. M., and Collett, J. L.: Fog water chemistry in Shanghai, Atmos. Environ., 45, 4034–4041, 2011.
Li, X., Li, P., Yan, L., Chen, J., Cheng, T., and Xu, S.: Characterization of polycyclic aromatic hydrocarbons in fog-rain events, J. Environ. Monitor., 13, 2988–2993, 2011.
Lin, T., Hu, L. M., Guo, Z. G., Qin, Y. W., Yang, Z. S., Zhang, G., and Zheng, M.: Sources of polycyclic aromatic hydrocarbons to sediments of the Bohai and Yellow Seas in East Asia, J. Geophys. Res., 116, D23305, doi:10.1029/2011jd015722, 2011.
Lindgren, F., Geladi, P., Berglund, A., Sjostrom, M., and Wold, S.: Interactive variable selection (Ivs) for Pls. 2. Chemical applications, J. Chemometr., 9, 331–342, 1995.
Liu, Y. N., Tao, S., Dou, H., Zhang, T. W., Zhang, X. L., and Dawson, R.: Exposure of traffic police to polycyclic aromatic hydrocarbons in Beijing, China, Chemosphere, 66, 1922–1928, 2007.
Ma, W. L., Li, Y. F., Qi, H., Sun, D. Z., Liu, L. Y., and Wang, D. G.: Seasonal variations of sources of polycyclic aromatic hydrocarbons (PAHs) to a northeastern urban city, China, Chemosphere, 79, 441–447, 2010.
Mai, B. X., Qi, S. H., Zeng, E. Y., Yang, Q. S., Zhang, G., Fu, J. M., Sheng, G. Y., Peng, P. N., and Wang, Z. S.: Distribution of polycyclic aromatic hydrocarbons in the coastal region off Macao, China: assessment of input sources and transport pathways using compositional analysis, Environ. Sci. Technol., 37, 4855–4863, 2003.
McWhinney, R. D., Zhou, S., and Abbatt, J. P. D.: Naphthalene SOA: redox activity and naphthoquinone gas–particle partitioning, Atmos. Chem. Phys., 13, 9731–9744, doi:10.5194/acp-13-9731-2013, 2013.
Mesquita, S. R., van Drooge, B. L., Reche, C., Guimarães, L., Grimalt, J. O., Barata, C., and Piña, B.: Toxic assessment of urban atmospheric particle-bound PAHs: relevance of composition and particle size in Barcelona (Spain), Environ. Pollut., 184, 555–562, 2014.
Miguel, A. H., Eiguren-Fernandez, A., Jaques, P. A., Froines, J. R., Grant, B. L., Mayo, P. R., and Sioutas, C.: Seasonal variation of the particle size distribution of polycyclic aromatic hydrocarbons and of major aerosol species in Claremont, California, Atmos. Environ., 38, 3241–3251, 2004.
Nemmar, A., Hoet, P. H. M., Vanquickenborne, B., Dinsdale, D., Thomeer, M., Hoylaerts, M. F., Vanbilloen, H., Mortelmans, L., and Nemery, B.: Passage of inhaled particles into the blood circulation in humans, Circulation, 105, 411–414, 2002.

ACPD
15, 20811–20850, 2015

Offenberg, J. H. and Baker, J. E.: Aerosol size distributions of polycyclic aromatic hydrocarbons in urban and over-water atmospheres, Environ. Sci. Technol., 33, 3324–3331, 1999.
Oliveira, C., Martins, N., Tavares, J., Pio, C., Cerqueira, M., Matos, M., Silva, H., Oliveira, C., and Camoes, F.: Size distribution of polycyclic aromatic hydrocarbons in a roadway tunnel in Lisbon, Portugal, Chemosphere, 83, 1588–1596, 2011.
Paatero, P. and Tapper, U.: Positive matrix factorization – a nonnegative factor model with optimal utilization of error-estimates of data values, Environmetrics, 5, 111–126, doi:10.1002/env.3170050203, 1994.
Pope, C. A., Ezzati, M., and Dockery, D. W.: Fine-particulate air pollution and life expectancy in the United States, New Engl. J. Med., 360, 376–386, 2009.
Poulain, L., Iinuma, Y., Müller, K., Birmili, W., Weinhold, K., Brüggemann, E., Gnauk, T., Hausmann, A., Löschau, G., Wiedensohler, A., and Herrmann, H.: Diurnal variations of ambient particulate wood burning emissions and their contribution to the concentration of Polycyclic Aromatic Hydrocarbons (PAHs) in Seiffen, Germany, Atmos. Chem. Phys., 11, 12697–12713, doi:10.5194/acp-11-12697-2011, 2011.
Ravindra, K., Sokhi, R., and Van Grieken, R.: Atmospheric polycyclic aromatic hydrocarbons: source attribution, emission factors and regulation, Atmos. Environ., 42, 2895–2921, 2008.
Sanderson, E. G. and Farant, J. P.: Atmospheric size distribution of PAHs: evidence of a high-volume sampling artifact, Environ. Sci. Technol., 39, 7631–7637, 2005.
Sheesley, R. J., Kruså, M., Krecl, P., Johansson, C., and Gustafsson, Ö.: Source apportionment of elevated wintertime PAHs by compound-specific radiocarbon analysis, Atmos. Chem. Phys., 9, 3347–3356, doi:10.5194/acp-9-3347-2009, 2009.
Shen, G., Wang, W., Yang, Y., Ding, J., Xue, M., Min, Y., Zhu, C., Shen, H., Li, W., Wang, B., Wang, R., Wang, X., Tao, S., and Russell, A. G.: Emissions of PAHs from indoor crop residue burning in a typical rural stove: emission factors, size distributions, and gas-particle partitioning, Environ. Sci. Technol., 45, 1206–1212, 2011.
Sofowote, U. M., McCarry, B. E., and Marvin, C. H.: Source apportionment of PAH in Hamilton Harbour suspended sediments: comparison of two factor analysis methods, Environ. Sci. Technol., 42, 6007–6014, 2008.
Theodosi, C., Grivas, G., Zarmpas, P., Chaloulakou, A., and Mihalopoulos, N.: Mass and chemical composition of size-segregated aerosols (PM_1, $PM_{2.5}$, PM_{10}) over Athens, Greece: local versus regional sources, Atmos. Chem. Phys., 11, 11895–11911, doi:10.5194/acp-11-11895-2011, 2011.

ACPD
15, 20811–20850, 2015

US EPA (U.S. Environmental Protection Agency): Risk assessment guidance for super fund volume I human health evaluation manual, part A, EPA/540/1-89/002, Office of Emergency and Remedial Response, Washington, D.C, USA, 1989.

van Drooge, B. L. and Ballesta, P. P.: Seasonal and daily source apportionment of polycyclic aromatic hydrocarbon concentrations in PM_{10} in a semirural European Area, Environ. Sci. Technol., 43, 7310–7316, 2009.

Venkataraman, C. and Friedlander, S. K.: Size distributions of polycyclic aromatic-hydrocarbons and elemental carbon. 2. Ambient measurements and effects of atmospheric processes, Environ. Sci. Technol., 28, 563–572, 1994.

Venkataraman, C., Lyons, J. M., and Friedlander, S. K.: Size distributions of polycyclic aromatic-hydrocarbons and elemental carbon, 1. sampling, measurement methods, and source characterization, Environ. Sci. Technol., 28, 555–562, 1994.

Venkataraman, C., Thomas, S., and Kulkarni, P.: Size distributions of polycyclic aromatic hydrocarbons – gas/particle partitioning to urban aerosols, J. Aerosol Sci., 30, 759–770, 1999.

Venkataraman, C., Negi, G., Sardar, S. B., and Rastogi, R.: Size distributions of polycyclic aromatic hydrocarbons in aerosol emissions from biofuel combustion, J. Aerosol Sci., 33, 503–518, 2002.

Wang, G., Kawamura, K., Xie, M., Hu, S., Gao, S., Cao, J., An, Z., and Wang, Z.: Size-distributions of *n*-alkanes, PAHs and hopanes and their sources in the urban, mountain and marine atmospheres over East Asia, Atmos. Chem. Phys., 9, 8869–8882, doi:10.5194/acp-9-8869-2009, 2009.

Wang, X., Chen, J., Cheng, T., Zhang, R., and Wang, X.: Particle number concentration, size distribution and chemical composition during haze and photochemical smog episodes in Shanghai, J. Environ. Sci.-China, 26, 1894–1902, 2014.

Wilson, J. G., Kingham, S., Pearce, J., and Sturman, A. P.: A review of intraurban variations in particulate air pollution: implications for epidemiological research, Atmos. Environ., 39, 6444–6462, 2005.

Wu, D., Wang, Z., Chen, J., Kong, S., Fu, X., Deng, H., Shao, G., and Wu, G.: Polycyclic aromatic hydrocarbons (PAHs) in atmospheric $PM_{2.5}$ and PM_{10} at a coal-based industrial city: implication for PAH control at industrial agglomeration regions, China, Atmos. Res., 149, 217–229, 2014.

Wu, S. P., Tao, S., and Liu, W. X.: Particle size distributions of polycyclic aromatic hydrocarbons in rural and urban atmosphere of Tianjin, China, Chemosphere, 62, 357–367, 2006.

ACPD
15, 20811–20850, 2015

Yang, H. H., Lai, S. O., Hsieh, L. T., Hsueh, H. J., and Chi, T. W.: Profiles of PAH emission from steel and iron industries, Chemosphere, 48, 1061–1074, 2002.
Yu, H. and Yu, J. Z.: Polycyclic aromatic hydrocarbons in urban atmosphere of Guangzhou, China: size distribution characteristics and size-resolved gas-particle partitioning, Atmos. Environ., 54, 194–200, 2012.
Yu, J. Z., Cocker, D. R., Griffin, R. J., Flagan, R. C., and Seinfeld, J. H.: Gas-phase ozone oxidation of monoterpenes: gaseous and particulate products, J. Atmos. Chem., 34, 207–258, 1999.
Zakaria, M. P., Takada, H., Tsutsumi, S., Ohno, K., Yamada, J., Kouno, E., and Kumata, H.: Distribution of polycyclic aromatic hydrocarbons (PAHs) in rivers and estuaries in Malaysia: a widespread input of petrogenic PAHs, Environ. Sci. Technol., 36, 1907–1918, 2002.
Zhang, K., Zhang, B. Z., Li, S. M., Wong, C. S., and Zeng, E. Y.: Calculated respiratory exposure to indoor size-fractioned polycyclic aromatic hydrocarbons in an urban environment, Sci. Total Environ., 431, 245–251, 2012a.
Zhang, K., Zhang, B. Z., Li, S. M., Wong, C. S., and Zeng, E. Y.: Calculated respiratory exposure to indoor size-fractioned polycyclic aromatic hydrocarbons in an urban environment, Sci. Total Environ., 431, 245–251, 2012b.
Zhang, R., Khalizov, A., Wang, L., Hu, M., and Xu, W.: Nucleation and growth of nanoparticles in the atmosphere, Chem. Rev., 112, 1957–2011, 2012.
Zhou, J. B., Wang, T. G., Zhang, Y. P., Mao, T., Huang, Y. B., Zhong, N. N., and Simoneit, B. R. T.: Sources and seasonal changes in the distributions of aliphatic and polycyclic aromatic hydrocarbons in size fractions of atmospheric particles of Beijing, China, Environ. Eng. Sci., 25, 207–220, 2008.

ACPD
15, 20811–20850, 2015

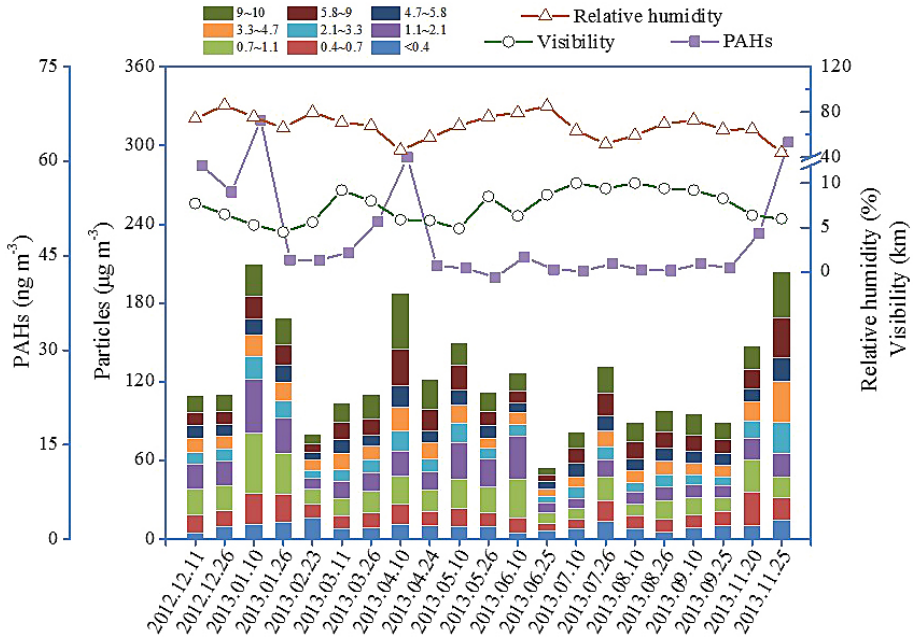

Figure 1. The sampling time series of PAH concentration (ng m^{-3}), size-segregated particles (μg m^{-3}), temperature (°C), visibility (km) and relative humidity (%).

ACPD
15, 20811–20850, 2015

Size distributions of polycyclic aromatic hydrocarbons in urban atmosphere

Y. Lv et al.

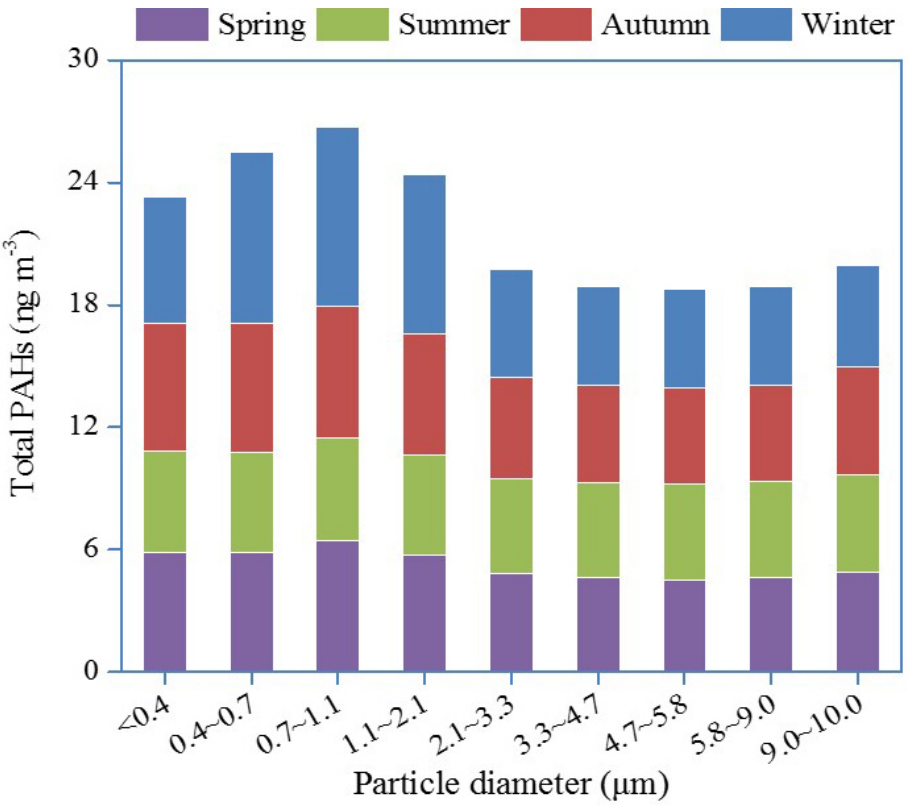

Figure 2. Seasonal variation of size-segregated total PAHs.

ACPD
15, 20811–20850, 2015

Size distributions of polycyclic aromatic hydrocarbons in urban atmosphere

Y. Lv et al.

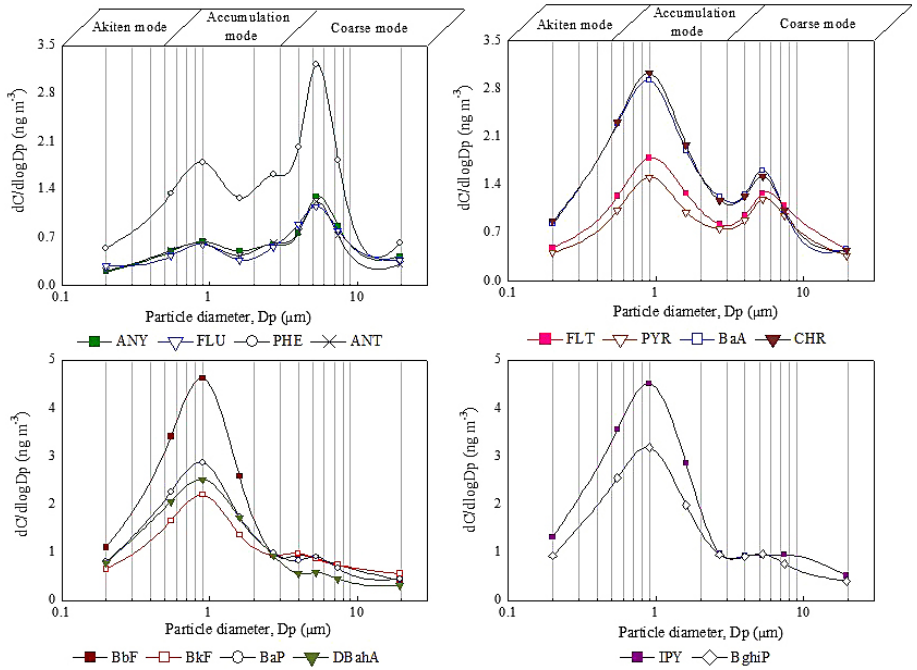

Figure 3. Size distributions of particle-bound PAHs (3 to 6 rings) in the atmosphere across one-year samples. dC is the concentration on each filter, C is the sum concentration on all filters, and dlogD_p is the logarithmic size interval for each impactor stage in aerodynamic diameter (D_p).

ACPD
15, 20811–20850, 2015

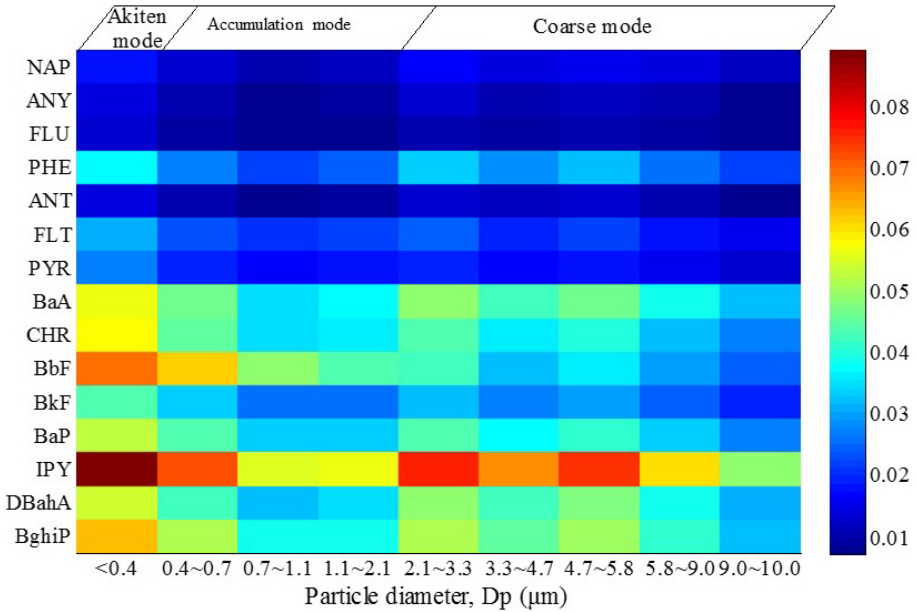

Figure 4. Mass Ratios of PAH species to size-segregated particles (ng μg^{-1}) across all samples.

ACPD
15, 20811–20850, 2015

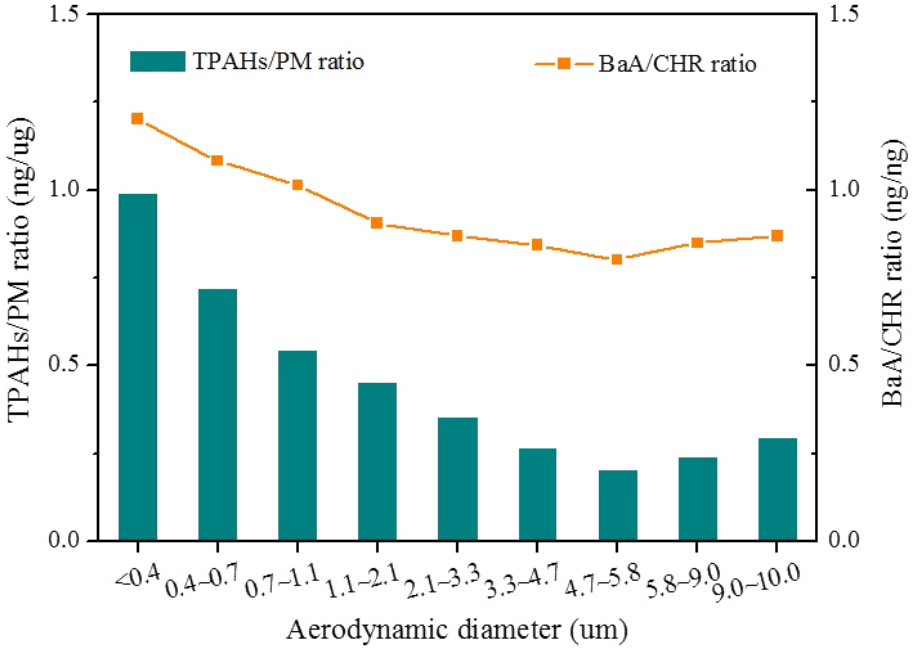

Figure 5. Ratios of total PAHs/size-segregated particles (ng μg^{-1}) and BaA/CHR across sizes (Sample time: 11 December 2012).

ACPD
15, 20811–20850, 2015

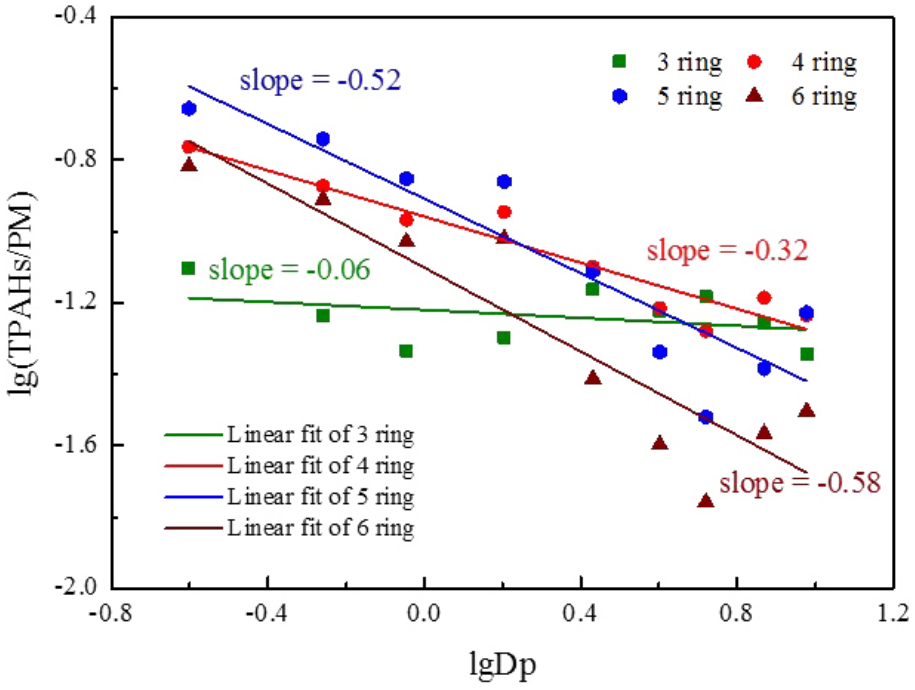

Figure 6. Plots of lg(TPAHs/PM) – lg(D_p) for PAHs with different ring number.

ACPD
15, 20811–20850, 2015

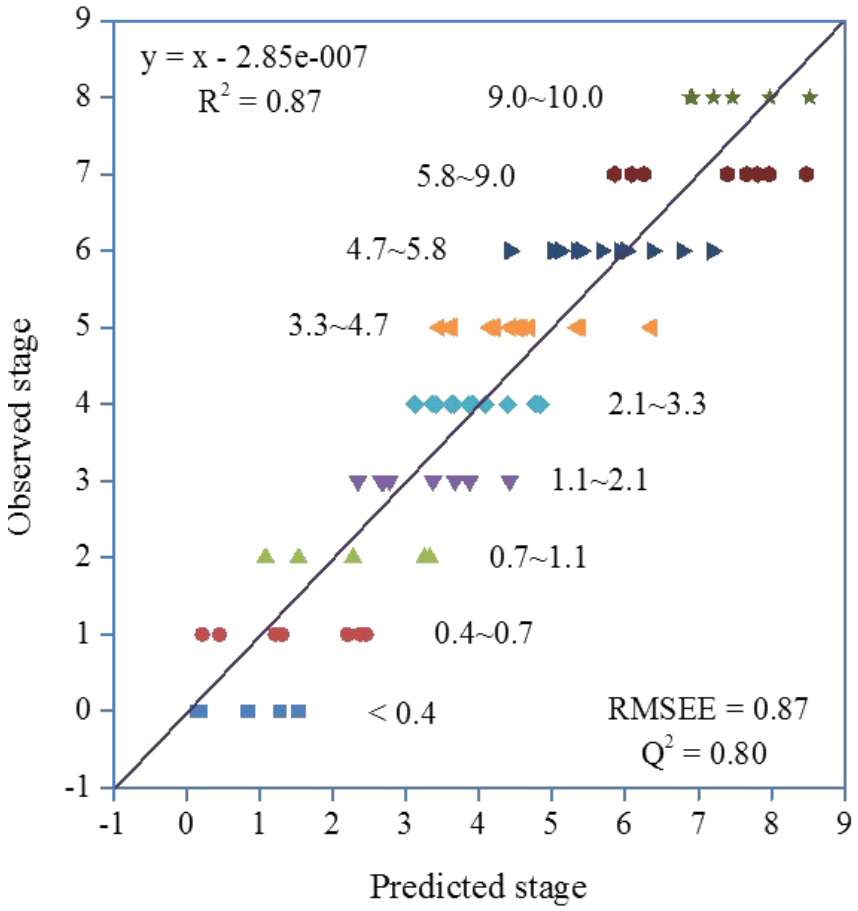

Figure 7. Measured and predicted total PAHs in all particles with sizes ranges from < 0.4 to 10 μm. The dashed line represents the 45° line.

ACPD
15, 20811–20850, 2015

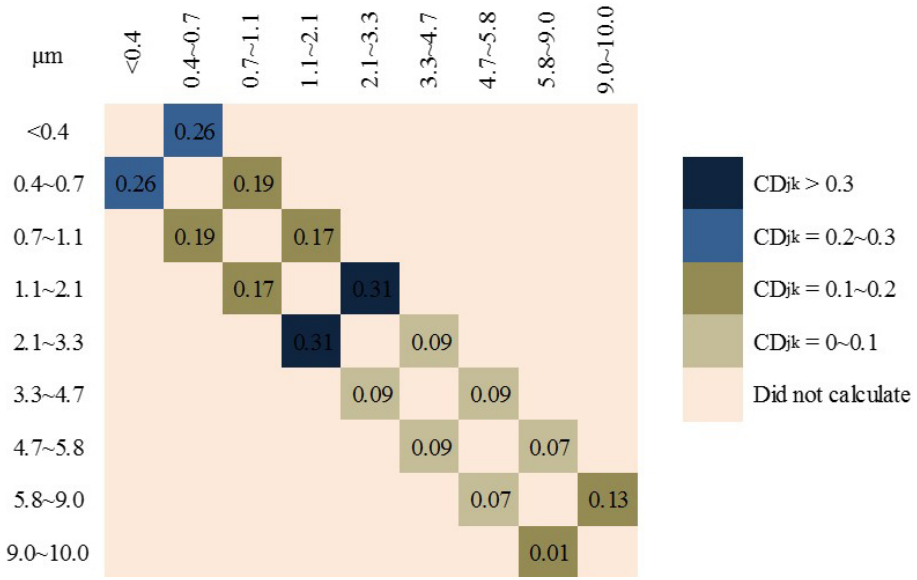

Figure 8. Similar comparison of PAHs profiles for the adjacent particles fractions.

ACPD
15, 20811–20850, 2015

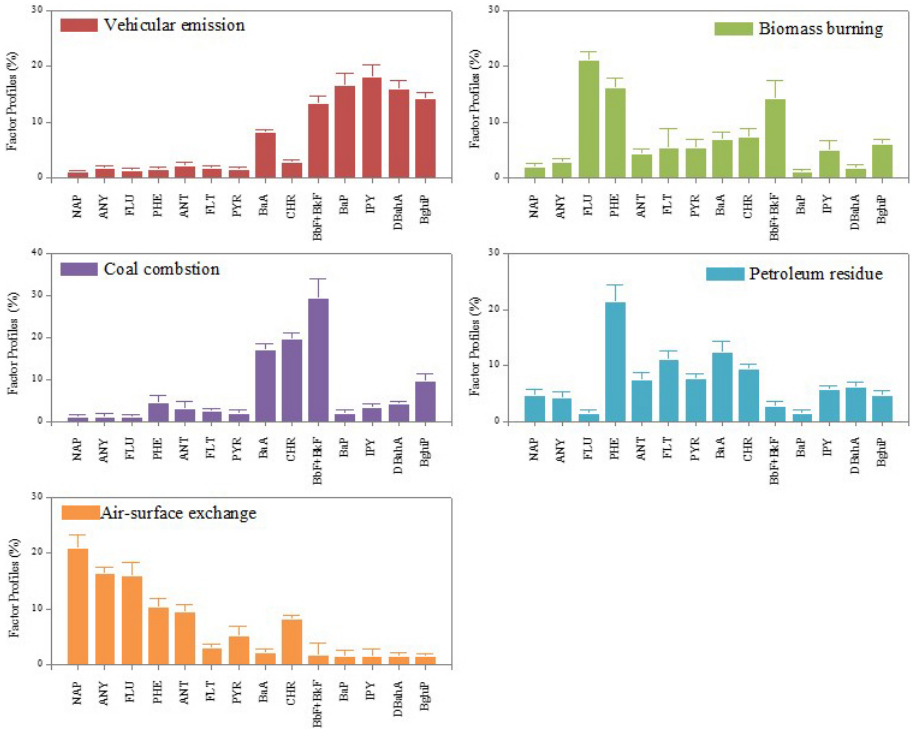

Figure 9. Profiles of the five factors resolved by the PMF model from full PAHs data set.

ACPD
15, 20811–20850, 2015

Size distributions of polycyclic aromatic hydrocarbons in urban atmosphere

Y. Lv et al.

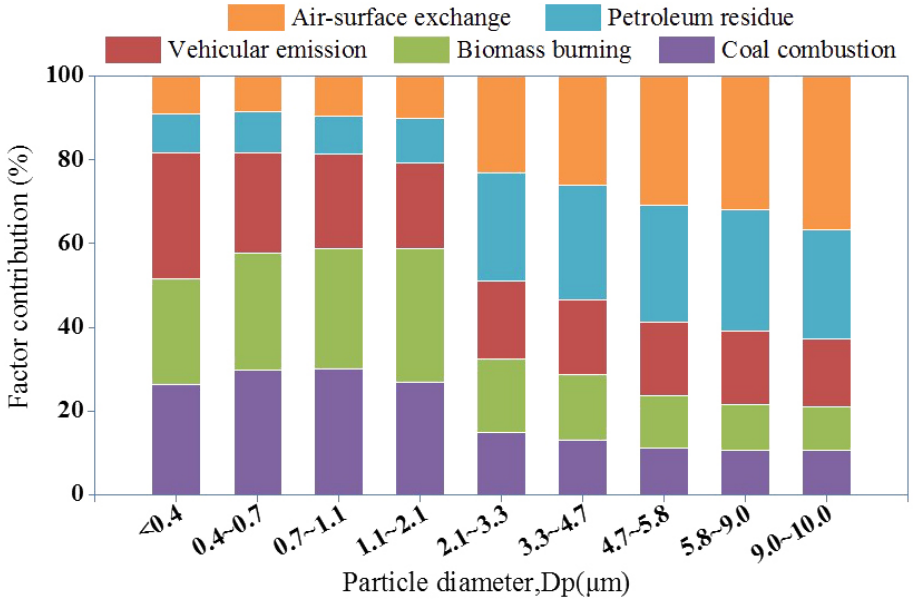

Figure 10. Factor contributions to size-segregated particles by the PMF model from full PAHs data set.

ACPD
15, 20811–20850, 2015

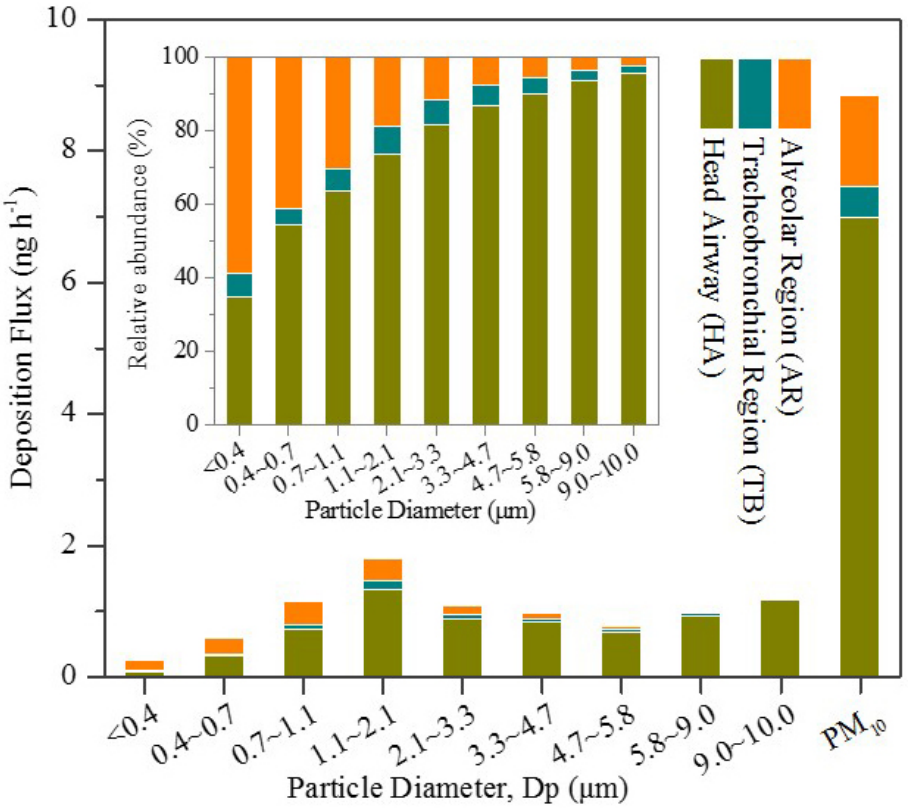

Figure 11. Deposition fluxes (estimated by ICRP model) and relative abundance of the size-segregated PAHs in the head airway, tracheobronchial, and alveolar region of the human respiratory tract.

ACPD
15, 20811–20850, 2015

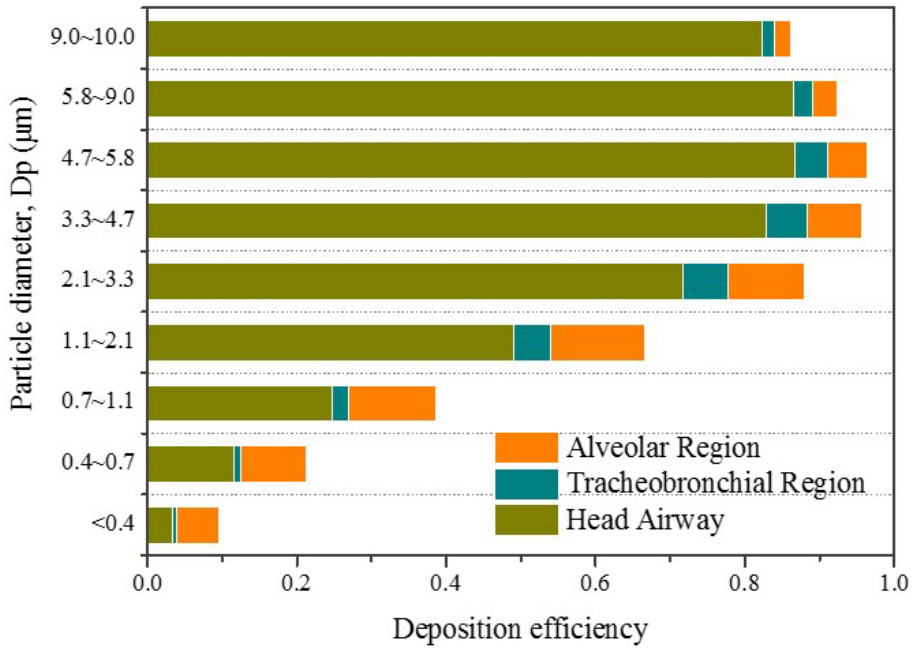

Figure 12. Deposition efficiencies (estimated by ICRP model) of the size-segregated PAHs in the head airway, tracheobronchial, and alveolar region.

ACPD
15, 20811–20850, 2015

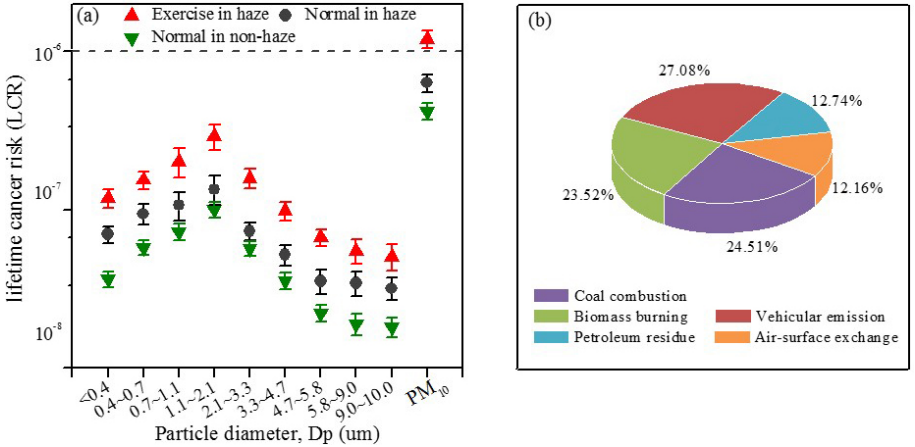

Figure 13. (a) Lifetime cancer risk (LCR) due to exposure to the size-segregated PAHs. PAHs through inhalation for normal and exercise people during haze and non-haze period. **(b)** Source contribution to total PAHs in PM_{10} during haze period by PMF analysis.

ACPD
15, 20811–20850, 2015